

Multi-component ground-based observation of ULF waves: goals and methods

Vjatcheslav A. Pilipenko⁽¹⁾, Massimo Vellante⁽²⁾, Sergey Anisimov⁽¹⁾, Marcello De Lauretis⁽²⁾,
Evgeniy N. Fedorov⁽¹⁾ and Umberto Villante⁽²⁾

⁽¹⁾ Institute of the Earth Physics, Moscow, Russia

⁽²⁾ Dipartimento di Fisica, Università dell'Aquila, Italy

Abstract

A revival of the combined magnetic and telluric electric measurements at magnetic observatories is suggested. A number of problems, where such observations might be very helpful, are outlined: 1) the account for the resonance structure of the ULF field during the magnetotelluric probing of low-conductive geoelectrical structures; 2) the hydromagnetic diagnostics of the magnetospheric plasma distribution; 3) the discrimination of ionospheric and seismic contributions in anomalous ULF signals possibly related with earthquakes. The experimental apparatus for telluric current measurements, which has recently been installed at the observatories of Borok (Russia) and L'Aquila (Italy), is described.

Key words *ULF waves – magnetic field line resonance – magnetotellurics – seismo-electromagnetic phenomena*

1. Introduction

Nowadays ULF variations (with time scales between 1 s and 10 min) of the terrestrial electromagnetic field are recorded on global network of observatories equipped with various kinds of magnetometers. These observations are one of the means for the continuous monitoring of dynamic phenomena in the magnetosphere, ionosphere, atmosphere and crust (Pilipenko, 1990). Earlier telluric observations of the electric component of ULF variations

were widely conducted, but up to now they have become very scarce due to larger noise level and industrial interference. Nonetheless, we believe that the revival of the combined magnetic and electric measurements might be very promising for many problems. In the present paper we discuss only some of them.

The practical application of the ground-based observations of ULF waves is mainly related to the magnetotelluric sounding (MTS) of the Earth's crust. From the point of view of MHD theory, the process of the typical day side Pc3-4 pulsations energy transport from an extra-magnetospheric source to the ground is inevitably related to the transformation of a compressional wave into an Alfvén field line oscillation. The fundamentals of this process form the basis of the resonance theory (Chen and Hasegawa, 1974; Southwood, 1974). This theory predicts a specific spatial structure of the ULF field near a resonant field line. On the

Mailing address: Dr. Vjatcheslav A. Pilipenko, Institute of the Earth Physics, B. Gruzinskaya 10, 123810 Moscow, Russia; e-mail: pilip@iephys.msk.su

other hand, for magnetotelluric models, the proper choice of the structure of the initial wave impinging the crust is of primary importance. The account for the resonance structure of the ULF field, verified by numerous experiments, may be significant for the MTS fundamentals (Pilipenko and Fedorov, 1993). In this paper we describe the numerical models which are used to examine the influence of the magnetospheric resonances on the accuracy of the standard MTS technique for various geoelectrical conditions.

Original MTS data, which include the records of magnetic and electric components of the ULF telluric field, can be used by the magnetospheric community for the development of new methods of hydromagnetic diagnostics of the magnetospheric plasma distribution (Guglielmi, 1989a,b). Here we further develop this new method and examine the range of its applicability. Hence hydromagnetic diagnostics could be enriched by coupling with telluric electric field data.

Recently, a blast of interest emerged in the study of anomalous signals in the ULF range possibly related with earthquakes (Fraser-Smith *et al.*, 1990; Molchanov *et al.*, 1992). Here we suggest some simple methods, based on combined electric and magnetic recordings, which may help to separate signals of ionospheric and seismic origin.

Lastly, we describe the experimental apparatus for telluric current measurements, in which the noise level is somewhat suppressed by means of special techniques. This experimental facility has recently been installed at the observatories of Borok (Russia) and L'Aquila (Italy) within the framework of a joint project.

2. Resonance effects in the spatial structure of ULF waves

2.1. Resonant structure of the ULF field

Below, we recall basic principles of the physics of ULF waves in the terrestrial environment. MHD disturbances from remote parts of the magnetosphere (for example, solar wind

disturbances, magnetopause surface waves, magnetosheath turbulence, etc.) propagate inside an inhomogeneous magnetosphere and, through a mode transformation, excite standing Alfvén oscillations of the Earth's magnetic field lines. Alfvén waves impinging the ionosphere are, in most cases, the sources of ULF geomagnetic pulsations (Pc3-5, Pi2) observed on the ground. The process of the mode transformation is most effective in the vicinity of the resonant geomagnetic shells where the local eigenfrequency $f_R(x)$ of Alfvén field line oscillations coincides with the frequency, f , of the external source. The mathematical description of the spatial structure of the field perturbation \mathbf{B} in the magnetosphere near resonant shells, according to the qualitative theory of differential equations (Kivelson and Southwood, 1986; Krylov *et al.*, 1981), can be expressed in the form of an asymptotic expansion in terms of the parameter $w = x - x_R(f) + i\delta_m$, where x is the coordinate of magnetic shells, $x_R(f)$ is the point where $f = f_R(x)$, δ_m is the width of the resonance region above the ionosphere and i is the imaginary unit. For the dipole geometry the solutions for the transverse magnetic components are (Lifshitz and Fedorov, 1986)

$$\begin{aligned} B_y^{(m)}(x, f) &= \\ &= B_0(f) \{ w^{-1} + \dots + C_1 \ln [ik_y (h_x/h_y)w] + \dots \} / h_y, \\ B_x^{(m)}(x, f) &= \\ &= B_0(f) \{ -ik_y \ln [ik_y (h_x/h_y)w] + \dots \} / h_y \end{aligned} \quad (2.1)$$

where y is the azimuthal coordinate, k_y denotes the azimuthal component of the wave vector, h_x and h_y are Lamé's coefficients. The expression (2.1) is, in fact, a generalization of the original simple «box model» of the magnetospheric resonator (Southwood, 1974; Chen and Hasegawa, 1974). The leading terms of the asymptotic expansion (2.1) and the expressions given by the «box field» model coincide, with the expense of some correction (the coefficient C_1 vanishes in the simple geometries with a constant curvature radius, as in Southwood (1974) and Radoski (1974).

The leading term in the asymptotic expression (2.1) which describes the resonant singularity of $B_y^{(m)}(x, f)$ near a resonant shell, *i.e.* when $|x - x_R(f)| \leq \delta_m$, can be presented in the form

$$B_y^{(m)}(x, f) = B_0(f) \frac{i\delta_m}{x - x_R(f) + i\delta_m}. \quad (2.2)$$

Due to the dissipation in the system the eigenfrequencies should contain an imaginary part: $\omega_A = 2\pi f_R \Rightarrow \omega_A - i\gamma$, where $\gamma > 0$. The resonance width δ_m is related to the damping rate γ by the relationship (Nishida, 1978)

$$\delta_m = -\gamma \left(\frac{\partial \omega_A}{\partial x} \right)^{-1}. \quad (2.3)$$

So, the sign of δ_m is determined by the sign of the gradient of the Alfvén frequency. Because throughout the magnetosphere (except at the plasmopause) $\partial \omega_A / \partial x < 0$, then $\delta_m > 0$. Based on the eq. (2.2) the meridional structure of the azimuthal component of the ULF field can be qualitatively represented as the combination of a «source» spectrum and a magnetospheric resonance response. The «source» part is related to a disturbance transported by a large-scale fast compressional wave and has a weak dependence on the x coordinate. The resonant magnetospheric response related to the Alfvén waves excitation is strongly localized and causes rapid variations of amplitude and phase when a resonant shell is crossed. The $B_x^{(m)}$ component, as (2.1) shows, has a weaker logarithmic singularity near the resonance, so the resonant behavior of this component would hardly be noticeable.

Upon transmission through the ionosphere, the horizontal spatial structure of ULF waves is distorted. This distortion can be analytically described for the Alfvén wave with spatial structure (2.2) transmitting through the «thin» ionosphere above an infinitely conductive ground. In the limit $k_y \ll k_x$ and $k_x h \gg 1$ (h being the height of the ionospheric E-layer) and when the interference of the incident wave and the wave reflected from the ground can be neglected (Alperovich and Fedorov, 1984), the

theory predicts that, on the ground, oscillations keep the same spatial form except for: a) a $\pi/2$ rotation: $B_y^{(m)} \rightarrow B_x$ (north-south component at the ground), $B_x^{(m)} \rightarrow B_y$ (east-west component at the ground) (Hughes and Southwood, 1976a,b); b) a smoothing of the resonance peak: $\delta = \delta_m + h$ (Alperovich *et al.*, 1991). So, the leading term (2.2) which describes amplitude and phase characteristics of the north-south ULF wave component at the ground can be approximately written in the form (Guglielmi, 1989a)

$$B_x(x, f) = \frac{B_R(f)}{1 - i\xi} \quad (2.4)$$

where $\xi = (x - x_R(f))/\delta$ denotes the normalized distance from the resonant point $x_R(f)$, $B_R(f)$ is the amplitude of the pulsation at the resonant point, and x is the coordinate of a magnetic shell, as measured at the ground from the equator along the geomagnetic meridian.

2.2. Magnetotellurics and resonant structure of the ULF field

The horizontal components of the magnetotelluric field, $\mathbf{E}_t = (E_x, E_y)$ and $\mathbf{B}_t = (B_x, B_y)$, recorded at the same point of the Earth's surface, are related through impedance condition. The surface impedance Z , in turn, is determined by the distribution of the crust's conductivity σ . In the 1D case, *i.e.* when lateral inhomogeneities in the electrical structure of the Earth's crust can be neglected, the magnetotelluric problem consists in the measurement of a $Z(\omega)$ and the restoration of a dependence of σ along depth z from the parametric dependence of impedance on frequency. The physical basis of MTS is the Tikhonov-Cagniard (T-C) model, which characterizes the ULF electromagnetic field over laterally homogeneous crust by an impedance coinciding with the impedance Z_g of a plane vertically propagating wave (Dmitriev and Berdichevsky, 1979; Wait, 1982). In this case the impedance relationship reduces to an extremely simple form

$$\mathbf{E}_t = -(Z_g/\mu_0) \mathbf{n} \times \mathbf{B}_t \quad (2.5)$$

where μ_0 is the magnetic permeability of free space and \mathbf{n} is the unit vector normal to the Earth's surface pointing downward.

Equation (2.5) is known in the theory of radiowave propagation over highly conductive surfaces as the Leontovich-Schelkunov boundary condition (or strong skin-effect approximation). If the field is homogeneous or linear over horizontal scales which are greater than the skin-depth d (i.e. $kd \ll 1$, where $d = \sqrt{2/\mu_0 \omega \sigma}$), then the T-C impedance Z_g can be applied (Wait, 1982). When the condition of the T-C model applicability breaks down the apparent impedance is determined not only by the geo-electrical properties of the underlying crust but also by the spatial structure of the incident ULF wave. For the resonant structure (2.1), (2.2), (2.4) of ULF pulsations the validity of strong skin-effect approximation can be reduced to the inequality $|k_g \delta| \gg 1$, where $k_g = (i\mu_0 \sigma \omega)^{1/2} = (1+i)/d$ is the wave vector in the ground. The value of d can be estimated with the numerical relationship d (km) = $[10 \rho$ ($\Omega \cdot \text{m}$) T (s)] $^{1/2}/2\pi$. The magnetospheric resonant effects may cause distortions of a standard MTS curve near a local resonant frequency which could be misinterpreted as a false feature of the Earth's crust structure (Alperovich *et al.*, 1991; Pilipenko and Fedorov, 1993). Distortion of the MTS curves by the resonant effects would be especially pronounced above low-conductive layers.

3. Modelling of the multi-component structure of the ULF field near the Earth's surface

A numerical model has been elaborated for the study of the influence of resonant effects on the structure of multi-component ULF field near the ground. The model is based on the analytical results on the transmission of a plane incident Alfvén wave through the «thin» ionosphere (Alperovich *et al.*, 1991; Alperovich and Fedorov, 1984). The spatial structure of the incident wave (i.e. the resonant structure described by (2.2)) is decomposed into spectral harmonics $\mathbf{B}(k_x, k_y)$ with spatial harmonic wave parameters k_x, k_y . The impedance condition for

a plane wave at the Earth's surface is analytically calculated with a recurrent formula for N homogeneous layers (Wait, 1982). The total fields $\mathbf{B}(x, y)$ and $\mathbf{E}(x, y)$ are then obtained by integrating the inputs of all harmonics.

The results of the numerical modelling will be presented for 3 cases. As a starting point we describe the multi-component wave structure at mid-latitudes above a highly conducting ground, corresponding to the situation of the mid-latitude Borok observatory. Then we consider the distortions of the wave structure above a low conductive ground, where the condition of strong skin-effect is violated. Finally, we present the expected ULF wave structure for the geo-electrical conditions typical for the low-latitude observatory of L'Aquila.

The incident Alfvén wave is assumed to have amplitude $B_y^{(m)} = 1$ nT. Typical day-side ULF waves have a much wider longitudinal extent with respect to the latitudinal extent, so azimuthal variations have been neglected, i.e. $k_y = 0$. Dayside ionospheric conductivities have been used, for which the Pedersen and Hall height-integrated conductivities are $\Sigma_p = 10$ mho,

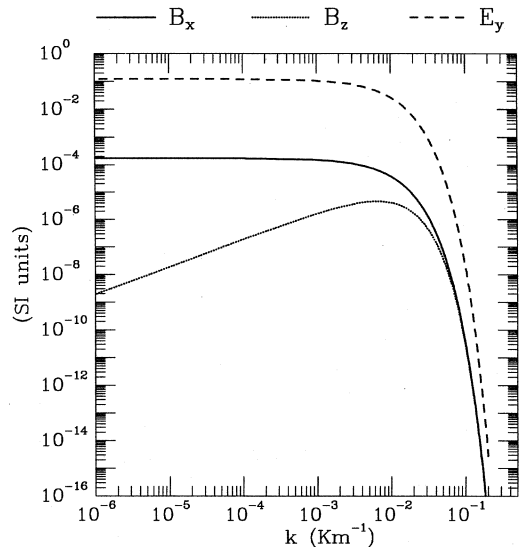


Fig. 1. The spatial spectrum of the ULF resonant structure above a high-conductive crust (Borok) with $\rho = 10 \Omega \cdot \text{m}$.

$\Sigma_H = 15$ mho. For a typical value of the Alfvén velocity in the magnetosphere $c_A = 800$ km/s, the magnetospheric wave conductivity Σ_A is much lower than ionospheric conductivities, *i.e.* $\Sigma_A = (\mu_0 c_A)^{-1} = 1$ mho. The height of the «thin» ionosphere is assumed to be $h = 100$ km and the resonance width above the ionosphere $\delta_m = 50$ km.

3.1. Case 1. Highly conductive ground (Borok observatory)

The ground resistivity of sedimentary layers in the region of the observatory is low: $\rho = 10 \Omega \cdot \text{m}$, so the validity of strong skin-effect condition is guaranteed: $|k_g \delta| \approx 13$. The geomagnetic latitude and inclination of the geomagnetic field are $\Phi = 55^\circ$ and $I = 70.7^\circ$, respectively. The resonant period is assumed to be $T_A = 100$ s.

The spatial spectrum of the ULF resonant structure, *i.e.* the dependencies $B_x(k)$, $B_z(k)$ and $E_y(k)$ on the horizontal wave number $k \equiv k_x$, are shown in fig. 1. The general form of these plots can be easily understood keeping in mind the Fourier transform of the singularity $(x + i\delta)^{-1}$: $F_k[(x + i\delta)^{-1}] \propto \exp(-k\delta)$ (for $k \geq 0$) and $F_k[(x + i\delta)^{-1}] = 0$ (for $k < 0$). As might be expected, for $k > \delta^{-1}$ the spectral densities of ULF components drop rapidly.

The spatial structure of the amplitudes of the ULF field components in the meridional direction near the resonant point is shown in fig. 2 (upper plot). To equal the scales of magnetic and electric components, the component E_y on the plot has been scaled by means of Z_g . As expected, both magnetic and electric horizontal components (which are practically indistinguishable in the figure) have a symmetrical maximum beneath the resonant field line ($x = 0$). The vertical component B_z is much less in magnitude, but it has a steeper maximum near the resonant point. The corresponding phase structure is shown in the bottom plot. Within the interval $x = \pm 500$ km, B_x and E_y exhibit a phase jump slightly less than 180° . Near the resonance point, the vertical magnetic component B_z has a two times steeper gradient than B_x . The phase shift between B_z and E_y

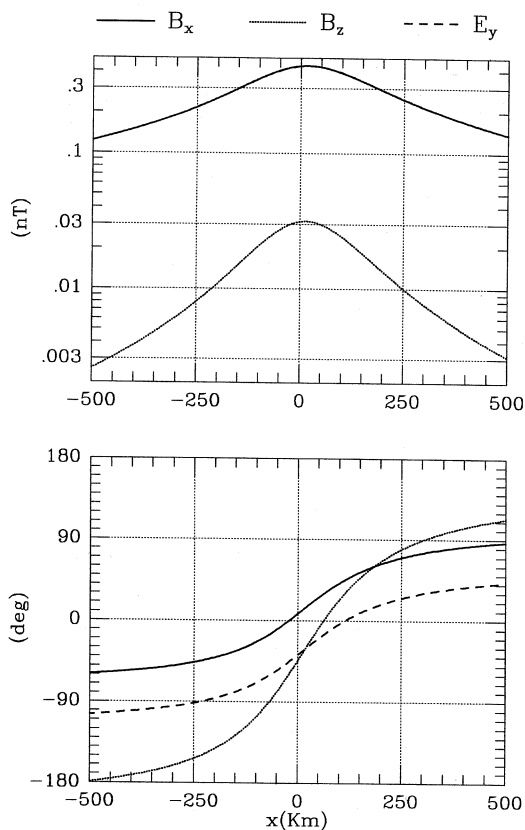


Fig. 2. The spatial structure in the meridional direction near the resonant point above a high-conductive crust (Borok) with $\rho = 10 \Omega \cdot \text{m}$. Upper plot: amplitudes; bottom plot: phases. Electric component E_y is scaled by Z_g .

changes from $-\pi/2$ up to $\pi/2$ at the other sides of the resonant peak. Just at the resonance point these components are in-phase. As we shall see later, this behaviour of the vertical magnetic component accords well to analytical approximations under the strong-skin-effect condition.

The amplitude and phase ratios between E_y and $H_x = B_x/\mu_0$, *i.e.* the impedance Z , are shown in fig. 3 (left panels). The amplitude is $\approx 8.9 \cdot 10^{-4} \Omega$, practically coincident with the known theoretical expression for the impedance of a plane wave over a homogeneous semi-space: $|Z_g| = (\omega\mu_0\rho)^{1/2}$.

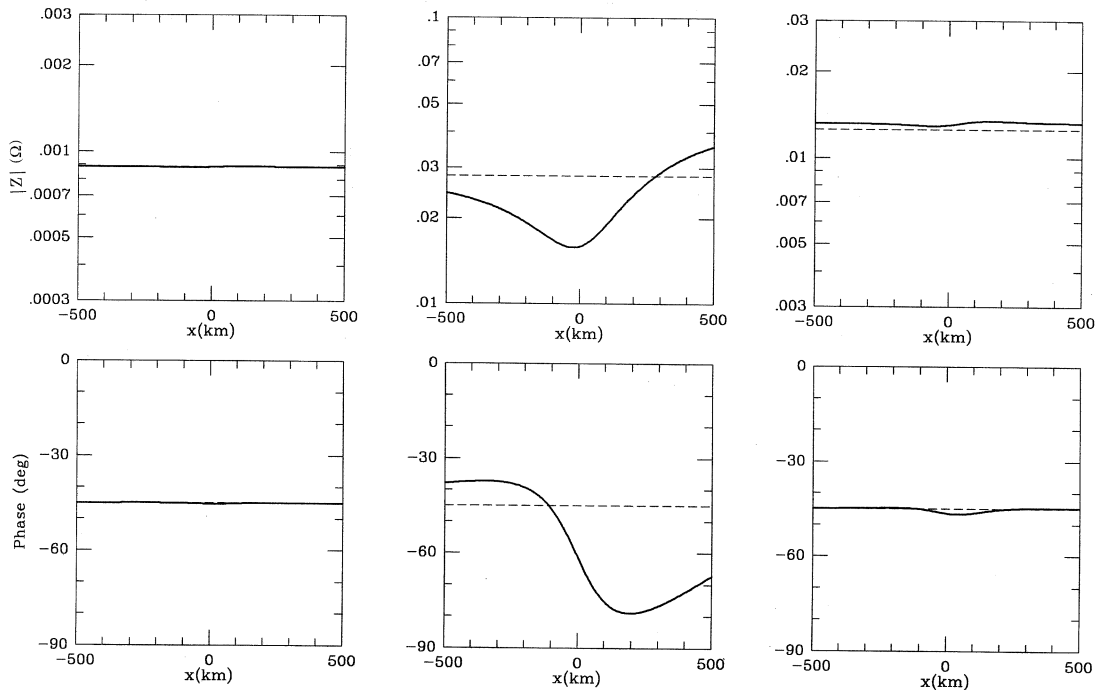


Fig. 3. The expected meridional variation (around the resonant point) of the amplitude (top) and phase (bottom) of the apparent impedance Z above: a high-conductive crust with $\rho = 10 \Omega \cdot \text{m}$ (Borok, left panels), a low-conductive crust with $\rho = 10^4 \Omega \cdot \text{m}$ (middle panels), a crust with $\rho = 300 \Omega \cdot \text{m}$ (L'Aquila, right panels). Dashed lines represent the theoretical T-C impedance values.

3.2. Case 2. Low-conductive ground

Now we consider the wave structure above a low-conductive crust with effective resistivity $\rho = 10^4 \Omega \cdot \text{m}$. The same parameters of the resonant structure, as in case 1, have been adopted. The estimates show that in this case the strong skin-effect condition is violated: $|k_g \delta| \approx 0.4$. This situation could be met, for example, above highly-resistive granites. In this case (fig. 4) the vertical magnetic component becomes comparable with the horizontal magnetic component. The meridional amplitude distribution is distorted compared with case 1. Moreover, this distortion differs for the magnetic and electric components. The phase meridional profile (fig. 4, bottom plot) is also distorted. In particular, the «synchronization point» between B_z and E_y is shifted about

100 km to the north. Hence, the various shifts and distortions of amplitude-phase profiles of B_x and E_y result in significant distortion of the apparent impedance Z (fig. 3, middle panels).

3.3. Case 3. Intermediate geoelectrical conditions (L'Aquila observatory)

Finally, we move to the description of the ULF wave structure at geoelectrical conditions corresponding to L'Aquila observatory. The inclination of the geomagnetic field is 58.5° . According to previous observations (Vellante *et al.*, 1989, 1996), the resonance period T_A is set equal to 15 s. Other magnetospheric and ionospheric parameters are the same as in cases 1, 2. According to previous magnetotelluric measurements (Palangio, private commu-

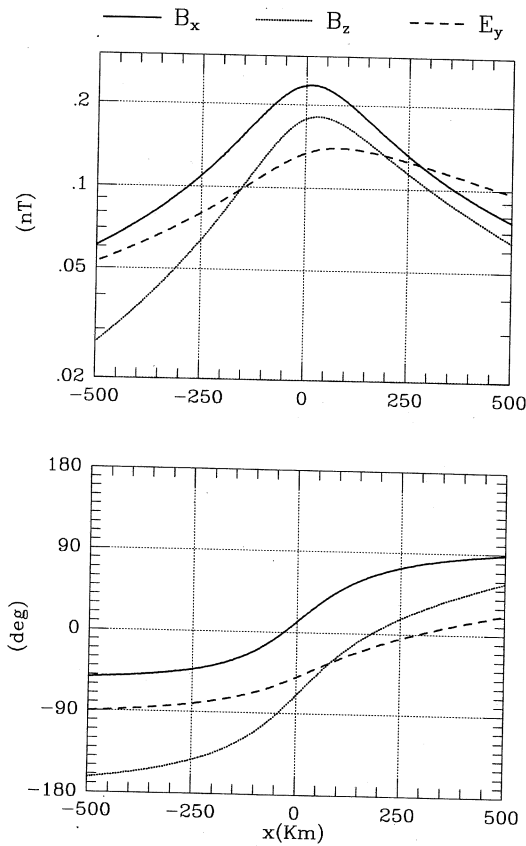


Fig. 4. The same as in fig. 2 but for a low-conductive crust ($\rho = 10^4 \Omega \cdot \text{m}$).

nication) the apparent resistivity in the Pc3 range is $\rho = 300 \Omega \cdot \text{m}$. The condition of a «good» conductor is still fulfilled: $|k_g \delta| \approx 6$. The same calculations as in cases 1 and 2, summarized in fig. 5 and fig. 3 (right panels), show that deviations from the structure over highly-conductive crust are rather small, though noticeable. The plots demonstrate another interesting effect: the shift of the meridional distribution from the projection of the resonant field line in the direction of phase velocity of pulsations. The physical sense of this effect, mentioned also by Alperovich *et al.* (1991), will be considered elsewhere.

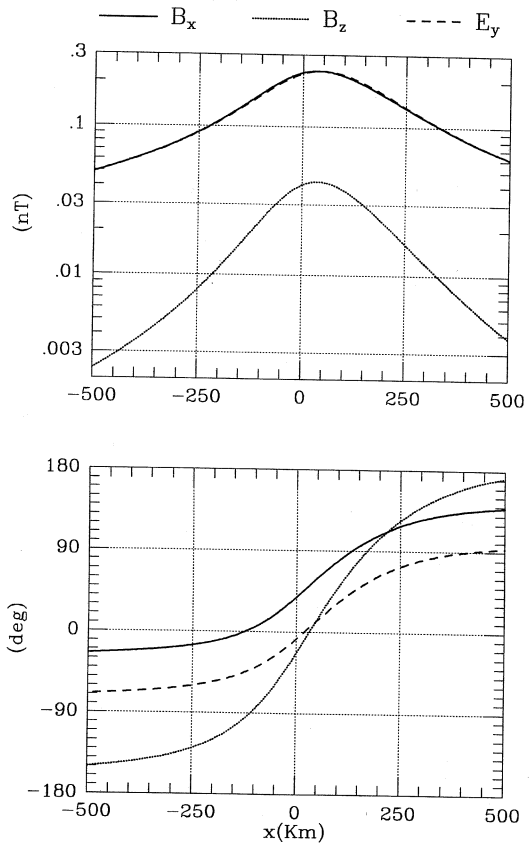


Fig. 5. The same as in fig. 2 but for L'Aquila geo-electrical conditions.

4. Diagnostics of the magnetospheric plasma with the data of ground-based ULF observations

For correct hydromagnetic diagnostics, effective and simple methods of operative determination of the resonant frequency distribution in a given region should be elaborated. Below we give a short summary of the existing methods of ground-based hydromagnetic diagnostics and describe in greater detail a recently proposed method, which uses both magnetic and electric components of the ULF field.

4.1. Gradient and polarization methods of the ULF resonant structure study

The principal problem of the experimental $f_R(x)$ determination consists in the fact that in most events, the input in the spectral content of ULF pulsations from resonant magnetospheric response and that from the «source» are comparable. So, in most cases, a spectral peak does not necessarily correspond to a local resonant frequency, and the width of a spectral peak cannot be directly used to determine the Q-factor of the magnetospheric resonator. This ambiguity can be resolved with the help of the experimental methods mentioned below, in particular the gradient method, proposed by Baransky *et al.* (1985). The measurements of gradients of spectral amplitude (desirably – phase also) at a small baseline exclude the influence of the source spectrum form and reveal even relatively weak resonant effects. The gradient method (Baransky *et al.*, 1985; Kurchashov *et al.*, 1987; Waters *et al.*, 1991) and its modifications (Green *et al.*, 1993; Gugliel’mi, 1992) allow estimation of resonant frequency of the field line between the stations and the width of the resonant peak δ . Despite the apparent simplicity of the one-dimensional resonance model described above, the theoretically predicted amplitude and phase meridional structure corresponds well to the experimental local structure of various types of ULF waves. The occurrence region of Alfvén resonances spreads from sub-auroral latitudes to rather low latitudes.

The different «sensitivity» of the various components of the ULF field to the magnetospheric Alfvén resonance means that the resonance frequency can be determined not only from the spatial structure, but also from the polarization properties of the ULF field. The polarization methods for the determination of $f_R(x)$ could supplement the gradient method, or even substitute it (Baransky *et al.*, 1990; Vellante *et al.*, 1993; Green *et al.*, 1993). As the eq. (2.1) show, the resonant response of the magnetosphere is characterized by a pronounced asymmetry of B_x and B_y components. At the same time, a source spectrum is imposed on both components in the same way.

Hence, even when a resonance response is masked by a source spectrum, the ratio $B_x(f)/B_y(f)$ (on the ground) should reveal a maximum at the resonant frequency. The gradient and polarization methods discriminated the resonant frequency from the complicated spectral content of low-latitude Pc3 pulsations (Pilipenko *et al.*, 1996).

4.2. Magnetospheric diagnostics with the use of the magnetic and electric ULF components

The vertical component of the ULF magnetic field is a sensitive indicator of inhomogeneities of both the ULF field and crust conductivity (Southwood and Hughes, 1978). So, the use of B_z data might be very promising for the elucidation of resonant features of the geomagnetic pulsation spatial structure. The relationship between vertical and horizontal magnetic components of the ULF field can be readily estimated in case of strong skin-effect. Then, the following relationship (Wait, 1982; Gugliel’mi, 1989a) can be used:

$$B_z = i(\mu_0 \omega)^{-1} (Z_g \operatorname{div} \mathbf{B}_\perp + \mathbf{B}_\perp \nabla Z_g). \quad (4.1)$$

For regions with laterally homogeneous conductivity of the Earth’s crust and for typical Pc3-5 and Pi2 pulsations the meridional gradient $\partial B_x / \partial x$ is the dominant term in the right hand side of (4.1). Using the form (2.4) of the resonant structure we obtain

$$B_z = - \frac{Z_g}{\mu_0 \omega \delta} \frac{B_x}{1 - i\xi}. \quad (4.2)$$

Under the considered conditions, as follows from (4.2), the resonant effects in the behaviour of the vertical component B_z might be even more pronounced than in the north-south component B_x . This fact is also supported by the results of numerical modelling (fig. 2).

The complex value of the surface impedance Z_g in eq. (4.2) can be excluded from consideration with the help of the impedance relation (2.5). Thus the relationship between B_z

and E_y is:

$$B_z/E_y = (1/\omega\delta)(1-i\xi)^{-1}. \quad (4.3)$$

Just at the frequency of an Alfvén resonance ($\xi = 0$) the ratio of spectral power densities $|B_z/E_y|$ should have a local maximum, and B_z and E_y should be in-phase. This prediction is supported by the numerical model (see fig. 6,

where the relevant spatial distributions are calculated for the Borok and L'Aquila geoelectrical conditions).

On the basis of the described properties of the vertical magnetic and east-west electric components of the ULF field an additional method of hydromagnetic diagnostics of the magnetosphere can be suggested. With this method it is possible to reconstruct the func-

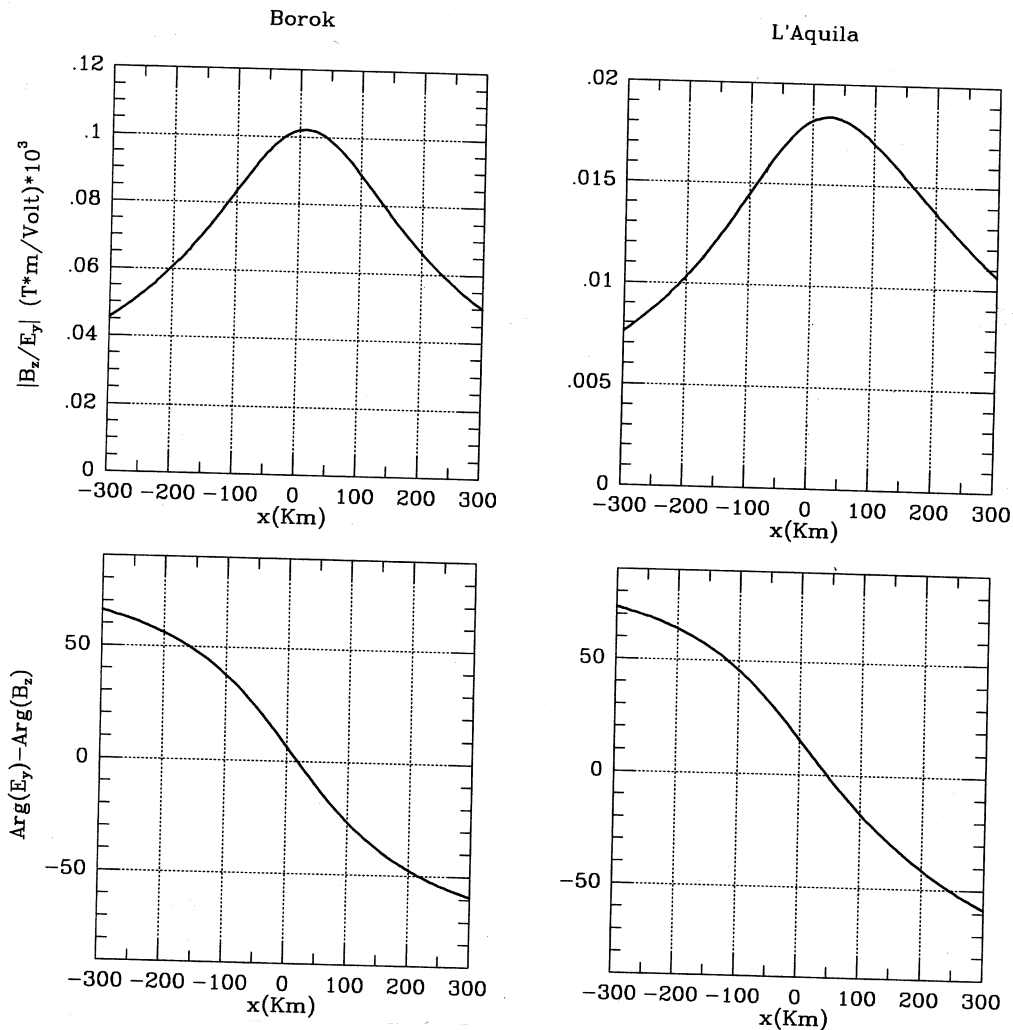


Fig. 6. The expected meridional variation of the ratio B_z/E_y (amplitude on the top and phase in the bottom) for Borok (left panels) and L'Aquila (right panels).

tional dependence $f_R(x)$ in the vicinity of the observation point, with the data from a single station (Gugliel'mi, 1989a). The distance between the observation point (x) and the resonant shell ($x_R(f)$) as well as the width of the resonance δ can be determined from (4.3) as

$$\begin{aligned} x - x_R &= -\omega^{-1} |E_y/B_z| \sin \psi \\ \delta &= \omega^{-1} |E_y/B_z| \cos \psi \end{aligned} \quad (4.4)$$

where $\psi = \text{Arg } E_y - \text{Arg } B_z$ is the phase difference between components. These relations make it possible to use multi-component data from a single site for the determination of the distance from the resonant field line at a given frequency. Reversing the dependence $x_R(f) \leftrightarrow f_R(x)$ the latitudinal variation of the resonant frequency $f_R(x)$ can be determined in the vicinity of the observation point. However, we should recall that this method for resonant frequency determination cannot be applied for low-conductive crust, where the condition of strong skin-effect is not valid.

5. Seismo-electromagnetic ULF disturbances

Studies of ULF magnetic disturbances in seismically active regions have revealed three classes of electromagnetic phenomena related with earthquakes:

a) Electromagnetic signals synchronous with the passage of seismic waves through the observation point from distant earthquakes (Eleman, 1965) or explosions (Anisimov *et al.*, 1985). These disturbances are caused by generation of currents when the conductor moves in the external magnetic field.

b) Sporadic magnetic impulses, slightly preceding (~ 10 s) seismic fronts (Belov *et al.*, 1974; Gokhberg *et al.*, 1989). Probably, these transient magnetic impulses are excited by the rapid movement of large-scale crust blocks during a quake. No profound theory of this process has been developed so far, besides some rough estimates of the effect (Gugliel'mi and Levshenko, 1994).

c) Irregular magnetic pulsations (Fraser-Smith *et al.*, 1990; Molchanov *et al.*, 1992) or sporadic impulses (Moore, 1964), observed tens of minutes-hours before strong earthquakes. This class of events is poorly studied and has no clear physical explanation. These anomalous ULF pulsations might be related with pre-shock seismic activity, with electro-magnetic radiation emitted by large-scale cracks during the final stage of crust destruction, with the induction effect of cracking-induced acoustic emission or with global coordinated systems of mechano-electrical transformers in the forthcoming fault (Gokhberg *et al.*, 1985).

The principal problem in the study of anomalous ULF disturbances related with seismic activity is the elaboration of effective algorithms to discriminate signals of different origin. The simultaneous use of both the magnetic and electric components of a signal under study might be an effective discrimination tool.

5.1. Effective impedances of seismo-magnetic signals

The induction effect of seismic waves can be estimated from Maxwell's quasi-stationary equations. The magnitude of the magnetic field B induced by the conductor oscillations in geomagnetic field B_0 is determined by Reynold's magnetic number $Re_m = \mu\sigma C_s \lambda_s = \pi^{-1}(\lambda_s/d)^2$, where C_s is the seismic wave velocity and λ_s is the wave length.

In the case $Re_m \gg 1$ («frozen-in» limit), the following estimate of the induced magnetic field can be obtained: $B/B_0 \simeq v/C_s \simeq \xi_s/\lambda_s$, where ξ_s and v are the displacement and the velocity of the medium associated to the seismic wave. In the reverse extreme case $Re_m \ll 1$ («diffusion» limit) the induced magnetic field can be estimated as $B/B_0 \simeq (v/C_s) Re_m$.

The electric field can be estimated from Faraday's induction equation $E \simeq C_s B$. However, this estimate of the electric field refers to the inertial reference system. If sensors oscillate with the Earth's surface, the transformation of electric field into laboratory system

should be taken into account: $\mathbf{E}' = \mathbf{E} + \mathbf{v} \times \mathbf{B}_0$. In the frozen-in limit, the electric fields in the inertial and the laboratory systems are of the same order. In the diffusion limit, the electric field in the laboratory system is determined by transformation factor, *i.e.* $E \approx v B_0$.

Neglecting the transformation effect, the apparent impedance of seismo-induction signals, *i.e.* the ratio of the electric component to the magnetic one, is determined by the velocity of the seismic wave (Gugliel'mi, 1989b)

$$Z_s \approx \mu C_s. \quad (5.1)$$

Contrary to this, the above ratio for ionospheric signals is equal to the T-C impedance Z_g . So, seismo-magnetic induction signals could be retrieved from ionosphere-magnetosphere ULF background based on its specific impedance features.

5.2. Impedance relationships for lithospheric signals

A similar idea could be applied for the possible discrimination between signals from ionospheric sources and underground sources. As a hint, let us consider the structure of electromagnetic disturbance at the boundary between air and crust in those two cases.

Any electromagnetic field which impinges the Earth's surface can be presented as a sum of plane waves of the form $\exp(-i\omega t + i\mathbf{k}_t \cdot \mathbf{r}) \{ \exp(i k_z z) + R \exp(-i k_z z) \}$, where R is the reflection coefficient. Both media are characterized by their characteristic resistance (or impedance) Z and wave vector k , which are determined by dielectric permeability ϵ and conductivity σ in the following way

$$Z = \sqrt{\mu / \tilde{\epsilon}}; \quad k = \omega \sqrt{\mu \tilde{\epsilon}}; \quad \tilde{\epsilon} = \epsilon + i\sigma / \omega. \quad (5.2)$$

Both media are considered to be non-magnetic, *i.e.* $\mu \equiv \mu_0$. The parameters in (5.2) are essentially different in the two media.

In the air, where $\sigma = 0$, $Z = Z_0 = \sqrt{\mu_0 / \epsilon_0} = 120\pi \Omega$ and $k = k_0 = \omega \sqrt{\mu_0 \epsilon_0} = \omega / c$.

In the ground, where $\sigma / (\epsilon \omega) \gg 1$, $k_g = \sqrt{i\omega \mu_0 \sigma}$, $Z = Z_g = \sqrt{\mu_0 \omega / i\sigma} = Z_0 (k_0 / k_g)$. At first glance it seems, as Hayakawa *et al.* (1993) believes, that electric and magnetic components of the wave in each medium must be related by the corresponding wave resistance, *e.g.*, Z_0 or Z_g . However, it is not the case near the Earth's surface where the primary and secondary waves are superposed.

In a laterally homogeneous layer the set of Maxwell's equations for plane waves is split into two groups for partial waves of electric and magnetic types. In electric (E-) mode $E_z \neq 0$ and $H_z = 0$, $\mathbf{E}_t \parallel \mathbf{k}_t$. This mode is excited by electric dipole. In magnetic (H-) mode $H_z \neq 0$ and $E_z = 0$, $\mathbf{H}_t \parallel \mathbf{k}_t$. This mode is excited by magnetic type source (loop current). Both modes in a layer are described by the same dispersion equation

$$k_z^2 + k_t^2 = i\omega \mu \tilde{\sigma} \quad (5.3)$$

where $\tilde{\sigma} = \sigma - i\omega \epsilon$.

Snelliu's law for the reflection and refraction of plane waves at a boundary reduces to the continuity of the transverse wave vector $k_t = (k_x, k_y)$. The surface partial impedances of electric and magnetic modes at the boundary between two homogeneous hemi-spaces are (Chetaev, 1984)

$$Z^{(E)} = \frac{-ik_z}{\tilde{\sigma}}; \quad Z^{(H)} = \frac{\omega \mu}{k_z}. \quad (5.4)$$

The ratio between electric and magnetic components at the boundary of two media is determined by the impedance of the medium where the wave will propagate. In the case of a ionospheric signal, which is incident on the highly-conductive Earth surface from above, the impedances of neither mode depend on the wave's spatial structure and reduce to the T-C impedance Z_g . For a wave from a probable lithospheric source, which impinges on the surface from the Earth's interiors, partial impedances of those modes are different and depend on the wave structure. For the E- and

H-mode these expressions are

$$Z_a^{(E)} = \frac{i|k_t|}{k_0} Z_0; \quad Z_a^{(H)} = \frac{k_0}{i|k_t|} Z_0. \quad (5.5)$$

The impedances of a signal from an underground source can be compared with ordinary T-C impedance of a signal from a ionospheric source

$$\frac{Z_a^{(E)}}{Z_g} = \frac{i|k_t|k_g}{k_0^2}; \quad \frac{Z_a^{(H)}}{Z_g} = \frac{k_g}{i|k_t|}. \quad (5.6)$$

For the reasonable parameters of a probable lithospheric source $|k_g| \geq |k_t| \gg k_0$, expression (5.6) shows that $|Z_a^{(E)}| \gg |Z_g|$ and $|Z_a^{(H)}| \geq |Z_g|$. Therefore the ratio of horizontal electric and magnetic components is essentially different for «ionospheric» and «lithospheric» signals, especially for the electric mode.

Thus, multi-component observations of the ULF field, including magnetic and electric components, may be effective in the discrimination between signals of ionospheric and seismic origins. Regular recording at ULF stations in seismo-active areas such as L'Aquila, could be used for monitoring both magnetospheric dynamics and seismic activity with the same data.

6. Experimental complex for multi-component ULF observations

The geomagnetic pulsation measuring system at L'Aquila consists of a triaxial high-sensitivity search coil magnetometer which has been operating almost continuously since 1983. Sensors are oriented along geographic north-south, east-west and vertical directions. The instrument transfer function is approximately linear for frequencies smaller than 0.3 Hz. On the high frequency side a rapid decrease of the transfer function removes the aliasing effects of the higher frequency components. A data processing unit samples the output voltage sig-

nals at 16 Hz; real time algorithms provide low-pass filtered data which are stored at a sampling rate of 1 Hz. More details about instrumentation and data reduction can be found in Cantarano *et al.* (1983) and Cerulli-Irelli *et al.* (1984). A low noise triaxial ring-core flux-gate magnetometer (variometer model LNV01, Nanotesla, Inc.) has also been operating at L'Aquila observatory since 1994. In order to investigate the scientific problems outlined in the previous sections, the geomagnetic pulsation facility at L'Aquila was recently integrated with an experimental apparatus for telluric current measurements. Threshold sensitivity of the geovoltmeter is about 0.01 mV/m for the distance between electrodes of 100 m. Bandwidth is 0.002-1 Hz, amplitude-frequency response in the given band is nearly flat. All data (three magnetic components from the search-coil magnetometer, three magnetic components from the flux-gate magnetometer and E_y) are stored at 1 Hz sampling rate by the same data acquisition system. System clock is periodically synchronized with standard radio transmission from DCF (Germany).

The basic experimental complex of Borok observatory has been developed for field digital recording of a wide class of geophysical signals. The experimental complex comprises the set of sensors, amplifiers, analog filters, clock and acquisition system. It gives the possibility to record variations in the frequency range 0.001-10 Hz of the following geophysical parameters: 3-component magnetic field with the use of induction magnetometers; atmospheric electric field with the help of an electrostatic fluxmeter; vertical atmospheric electric current by the current collector; atmospheric pressure by microbarograph. Also multi-frequency Doppler sounding of the ionosphere and riometric observations of cosmic radio noise absorption at frequency 32 MHz are operating. For the study of multi-component structures of the ULF field, this complex has been supplemented with the 3-component telluric current measurements using 300 m baseline between lead electrodes and 400 m borehole. The on-line digital recordings of any geophysical field are performed with the use of PC computer or analog-digital converter.

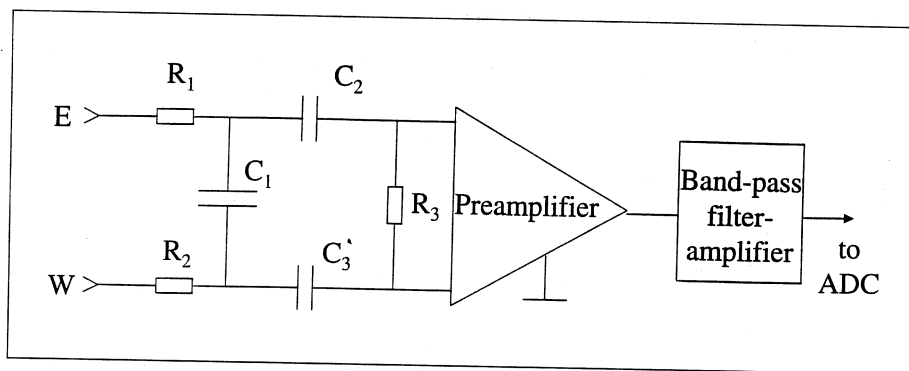


Fig. 7. Block diagram of the telluric electric field measuring system.

The observations of telluric currents require high sensitivity and the enhanced noise-defense of measuring installation. This is required to study fine effects such as: resonant features of ULF field structure, anomalous seismo-electromagnetic activity, etc. The practical measurements are usually conducted under anthropogenic electromagnetic conditions, including industrial, communication and traffic interferences. In order to suppress the in-phase noise, a symmetrical scheme (fig. 7) with differential input is used both at L'Aquila and Borok. The geovoltmeter comprises high-impedance differential measuring amplifier, two measuring and one common lead electrodes.

7. Conclusions

All the potentialities of the combined application of the gradient and the polarization methods to restore the meridional structure of the plasma density in the magnetosphere have still not been achieved. The new method of hydromagnetic diagnostics which uses the multi-component structure of a magnetotelluric field seems promising. It would be particularly interesting to compare the application of these methods for the study of resonant effects at low and middle latitudes.

For the illustration of possible effects we considered a simplified situation: no east-west

variations ($k_y = 0$), vertically homogeneous crust, etc. However, with the help of an elaborated numerical model more complicated cases could be treated. The preliminary analysis with the use of this numerical model would be especially important to perform MTS in the regions with low-conductive layers. For a correct interpretation of MTS curves a preliminary analysis of possible distortions caused by magnetospheric resonance effects should be made.

It is widely believed that electromagnetic methods will play a key role in the operative forecasting of earthquake risk. This research would be more effective if some criteria for the separation of signals of different nature are used. Even the current rough knowledge of the physics of seismo-electromagnetic phenomena suggests some of these criteria. The realization of the discrimination methods would require only elaboration of simple algorithms for real-time analysis of the apparent impedances of detected ULF signals. All the problems outlined in this paper can be studied with the same set of magnetic and electric ULF data.

Acknowledgements

This research was supported by INTAS (grant # 93-3412).

REFERENCES

- ALPEROVICH, L.S. and E.N. FEDOROV (1984): Propagation of hydromagnetic waves through the ionospheric plasma and spatial characteristics of geomagnetic variations, *Geomagn. Aeron.*, **24**, 650-657.
- ALPEROVICH, L.S., E.N. FEDOROV and T.B. OS'MAKOVA (1991): About peculiarities of a telluric field near resonant magnetic shell, *Izv. Akad. Nauk SSSR, Fiz. Zemli*, **N7**, 60-71.
- ANISIMOV, S.V., M.B. GOKHBERG, E.A. IVANOV, M.N. PEDANOV, N.N. RUSAKOV, V.A. TROITSKAYA and V.I. GONCHAROV (1985): Short-period oscillations in the Earth's magnetic field during an industrial explosion, *Dokl. Akad. Nauk SSSR*, **281**, 556-559.
- BARANSKY, L.N., YU.E. BOROVKOV, M.B. GOKHBERG, S.M. KRYLOV and V.A. TROITSKAYA (1985): High resolution method of direct measurement of the magnetic field line's eigenfrequencies, *Planet. Space Sci.*, **33**, 1369-1374.
- BARANSKY, L.N., S.P. BELOKRIS, YU.E. BOROVKOV and C.A. GREEN (1990): Two simple methods for the determination of the resonance frequencies of magnetic field lines, *Planet. Space Sci.*, **38**, 1573-1576.
- BELOV, S.V., N.I. MIGUNOV and G.A. SOBOLEV (1974): Magnetic effects accompanying strong earthquakes in Kamchatka, *Geomagn. Aeron.*, **14**, 380-382.
- CANTARANO, S., P. CERULLI-IRELLI, A. EGIDI, R. ORFEI, M. VELLANTE and U. VILLANTE (1983): A facility for measuring geomagnetic micropulsations at L'Aquila, Italy, *Il Nuovo Cimento*, **6C**, 40-48.
- CERULLI-IRELLI, P., A. EGIDI, R. ORFEI, M. VELLANTE and U. VILLANTE (1984): Preliminary measurements of geomagnetic micropulsations at L'Aquila, Italy, *Il Nuovo Cimento*, **7C**, 1-8.
- CHEN, L. and A. HASEGAWA (1974): A theory of long-period magnetic pulsations. 1. Steady state excitation of field line resonance, *J. Geophys. Res.*, **79**, 1024-1032.
- CHETAEV, D.N. (1984): *Directional Analysis of Geomagnetic Pulsations*, Moscow, p. 228 (in Russian).
- DMITRIEV, V.I. and M.N. BERDICHEVSKY (1979): Fundamental model of magnetotelluric sounding, *IEEE*, **67**, 69-79.
- ELEMAN, F. (1965): The response of magnetic instruments to earthquake waves, *J. Geomagn. Geoelectr.*, **18**, 43-72.
- FRASER-SMITH, A.C., A. BERNARDI, P.R. MCGILL, R.E. LADD, R.A. HELLIWELL and O.G. VILLARD (1990): Low frequency magnetic field measurements near the epicenter of the $M_s = 7.1$ Loma Prieta earthquake, *Geophys. Res. Lett.*, **17**, 1465-1468.
- GOKHBERG, M.B., I.L. GUFELD, N.I. GERSHENZON and V.A. PILIPENKO (1985): Electromagnetic effects during the destruction of the Earth's crust, *Izv. Akad. Nauk SSSR, Fiz. Zemli*, **1**, 72-87.
- GOKHBERG, M.B., S.M. KRYLOV and V.T. LEVSHENKO (1989): Electromagnetic field of the earthquake focus, *Dokl. Akad. Nauk SSSR*, **308**, 62-65.
- GREEN, A.W., E.W. WORTHINGTON, L.N. BARANSKY, E.N. FEDOROV, N.A. KURNEVA, V.A. PILIPENKO, D.N. SHVETZOV, A.A. BEKTEMIROV and E. PHILIPOV (1993): Alfvén field line resonances at low latitudes ($L = 1.5$), *J. Geophys. Res.*, **98**, 15693-15699.
- GUGLIELMI, A.V. (1989a): Diagnostics of the plasma in the magnetosphere by means of measurement of spectrum of Alfvén oscillations, *Planet. Space Sci.*, **37**, 1011-1012.
- GUGLIELMI, A.V. (1989b): Hydromagnetic diagnostics and geoelectric exploration, *Usp. Fiz. Nauk*, **158**, 605-637.
- GUGLIELMI, A.V. (1992): Hydromagnetic diagnostics of the space environment, *Izv. Akad. Nauk SSSR, Fiz. Zemli*, **5**, 45.
- GUGLIELMI, A.V. and V.T. LEVSHENKO (1994): Electromagnetic signals from earthquakes, *Izv. Akad. Nauk SSSR, Fiz. Zemli*, **5**, 65-70.
- HAYAKAWA, M., I. TOMIZAWA, K. OHTA, S. SHIMAKURA, Y. FUJINAWA, T. TAKAHASHI and T. YOSHINO (1993): Direction finding of precursory radio emissions associated with earthquakes: a proposal, *Phys. Earth Planet. Inter.*, **77**, 127-135.
- HUGHES, W.J. and D.J. SOUTHWOOD (1976a): The screening of micropulsation signals by the atmosphere and ionosphere, *J. Geophys. Res.*, **81**, 3234-3240.
- HUGHES, W.J. and D.J. SOUTHWOOD (1976b): An illustration of modification of geomagnetic pulsation structure by the ionosphere, *J. Geophys. Res.*, **81**, 3241-3247.
- KIVELSON, M.G. and D.J. SOUTHWOOD (1986): Coupling of global magnetospheric MHD eigenmodes to field line resonances, *J. Geophys. Res.*, **91**, 4345-4351.
- KRYLOV, A.L., A.E. LIFSHITZ and E.N. FEDOROV (1981): About resonant properties of the magnetosphere, *Izv. Akad. Nauk SSSR, Fiz. Zemli*, **6**, 49-59.
- KURCHASHOV, YU.P., YA.S. NIKOMAROV, V.A. PILIPENKO and A. BEST (1987): Field line resonance effects in local meridional structure of mid-latitude geomagnetic pulsations, *Ann. Geophys.*, **5A**, 147-154.
- LIFSHITZ, A.E. and E.N. FEDOROV (1986): Hydromagnetic oscillations of the magnetosphere-ionosphere resonator, *Dokl. Akad. Nauk SSSR*, **287**, 90.
- MOLCHANOV, O.A., YU.A. KOPYTENKO, P.M. VORONOV, E.A. KOPYTENKO, T.G. MATIASHVILI, A.C. FRASER-SMITH and A. BERNARDI (1992): Results of magnetic field measurements near the epicenters of the Spitak ($M_s = 6.9$) and Loma Prieta ($M_s = 7.1$) earthquakes: comparative analysis, *Geophys. Res. Lett.*, **19**, 1495-1498.
- MOORE, G.W. (1964): Magnetic disturbances preceding the 1964 Alaska earthquake, *Nature*, **203**, 508-509.
- NISHIDA, A. (1978): *Geomagnetic Diagnosis of the Magnetosphere* (Springer, Berlin), pp. 256.
- PILIPENKO, V.A. (1990): ULF waves on the ground and in space, *J. Atmos. Terr. Phys.*, **52**, 1193-1209.
- PILIPENKO, V.A. and E.N. FEDOROV (1993): Magnetotelluric sounding of the crust and hydromagnetic monitoring of the magnetosphere with the use of ULF waves, *Ann. Geofis.*, **36** (5-6), 19-33.
- PILIPENKO, V.A., M. VELLANTE and K. YUMOTO (1996): Ground-based monitoring of the magnetospheric plasma by ULF hydromagnetic spectroscopy, in *XXI EGS General Assembly*, Hague.
- RADOSKI, H.R. (1974): A theory of latitude dependent geomagnetic micropulsations: the asymptotic fields, *J. Geophys. Res.*, **79**, 595-603.

- SOUTHWOOD, D.J. (1974): Some features of field line resonances in the magnetosphere, *Planet. Space Sci.*, **22**, 483-491.
- SOUTHWOOD, D.J. and W.J. HUGHES (1978): Source induced vertical components in geomagnetic pulsation signals, *Planet. Space Sci.*, **26**, 715-720.
- VELLANTE, M., U. VILLANTE, M. DE LAURETIS and P. CERULLI-IRELLI (1989): An analysis of micropulsation events at a low-latitude station during 1985, *Planet. Space Sci.*, **37**, 767-773.
- VELLANTE, M., U. VILLANTE, R. CORE, A. BEST, D. LENNERS and V.A. PILIPENKO (1993): Simultaneous geomagnetic pulsation observations at two latitudes: resonant mode characteristics, *Ann. Geophys.*, **11**, 734-741.
- VELLANTE, M., U. VILLANTE, M. DE LAURETIS and G. BARCHI (1996): Solar cycle variation of the dominant frequencies of Pc3 geomagnetic pulsations at $L = 1.6$, *Geophys. Res. Lett.*, **23**, 1505-1508.
- WAIT, J.R. (1982): *Geoelectromagnetism* (Academic Press).
- WATERS, C.L., F.W. MENK, B.J. FRASER and P.M. OSTWALD (1991): Phase structure of low-latitude Pc3-4 pulsations, *Planet. Space Sci.*, **39**, 569-582.

(received November 24, 1997;
accepted February 20, 1998)